ROLE OF NON-EQUILIBRIUM VACANCIES IN SPINODAL DECOMPOSITION

N.V. TYUTYUNNYK, A.N. GUSAK

Cherkasy National University
(81, Shevchenko Blvd., Cherkasy 18031, Ukraine; e-mail: nadushenka@ukr.net, amgusak@ukr.net)

PACS 66.30.-h

The standard Cahn–Hilliard model of spinodal decomposition has an essential fault, because it uses the approximation of equilibrium vacancies, which is valid only for processes with a characteristic length larger than the mean free path of vacancies. A procedure for the consideration of a non-equilibrium redistribution of vacancies at the spinodal decomposition and its influence on the decomposition kinetics is proposed. The hierarchy of characteristic times for the evolution of the morphology and the concentration is analyzed for a two-dimensional system.

1. Introduction

Initial stages of the spinodal decomposition were elegantly described by Hillert [1] and Cahn and Hilliard [2]. In this case, the nonlocal interactions corresponding to gradient terms in the equation for the Gibbs free energy density for inhomogeneous alloys were taken into account. Since the middle of the 1990s, the three-dimensional atomic tomography made it possible to experimentally study the details of an alloy structure in the course of spinodal decay [3]. This technique enables both the structure and the distribution of concentrations to be analyzed simultaneously. In their classical theory, Cahn and Hilliard (CH) obtained the optimum parameters of a lamellar structure, making allowance for the gradient terms and the elastic energy for an inhomogeneous alloy. They used a modified thermodynamics, but in the framework of the standard kinetic approach, by applying the Darken approach [4] for the description of the diffusion redistribution between lamellae.

The basic Darken assumption consists in admitting a strictly equilibrium concentration of vacancies, everywhere and at every time. A probable influence of nonequilibrium defects on the kinetics and the result of the spinodal decomposition were analyzed much later. In particular, the spinodal decomposition in a thin film with a periodic distribution of dislocations over the surfaces was studied by Hu and Chen [5]. They developed a phase field model for simulating the influence of periodically distributed interfacial dislocations on the process of spinodal decomposition in a confined film. The results of work [5] showed that the dislocation-induced stresses give rise to a directional spinodal decomposition. A probable influence of nonequilibrium vacancies on the spinodal decomposition was examined for the first time in work [6].

After the works by Nazarov, Gurov, and others [7–9], it became evident that the Darken approximation is valid only if the mean free path of vacancies (from a source to a sink) is much shorter than the characteristic diffusion length of the problem. A more detailed analysis of this problem was presented by Fischer and Svoboda [10]. In that work, the vacancy concentration coincides with the equilibrium one only on the surface of a multicomponent layer acting as an ideal source and a sink for vacancies (in works [6,8], the vacancy sources and sinks are considered as "smeared" over the volume).

The relaxation kinetics of vacancies at the spinodal decomposition was also taken into account in a recently proposed approach of self-consistent mean field [11]. In the case of the mutual diffusion, the characteristic diffusion length is simply the width of a diffusion zone. In the case of the spinodal decomposition, especially at its initial stage, the characteristic diffusion length is the period of a lamellar structure, i.e. its magnitude does not exceed tens of nanometers. This value is much shorter than the characteristic mean free path of vacancies in real alloys, which, as a rule, is of a micron order. Therefore, while describing the emergence of a lamellar structure,

it is necessary to consider a nonequilibrium redistribution of vacancies between lamellae, which is induced by the difference between the partial diffusion coefficients of components.

Really, let the mobility of atoms B be higher than that of atoms A. Then, when the components are separated in the course of spinodal decomposition, the initial diffusion flux of atoms B directed toward the band of the "future" beta-phase has to be larger than the inverse flux of atoms A toward the band of the "future" alpha-phase. This means that the vacancy flux from the beta-band into the alpha-one must emerge. Hence, there must arise the vacancy oversaturation in the "future" alpha-phase and the vacancy undersaturation in the "future" beta-phase. In other words, not only a wave of basic components, A and B, emerges, but also of vacancies. As we will see below, not all redundant vacancies have enough time to migrate to sinks for the characteristic decomposition time, which means that the local gradients of vacancy concentrations cannot be neglected in the diffusion equation. According to the general Le Chatelier–Braun damping principle, the emergence of a nonequilibrium vacancy distribution must slow down the decomposition. The specific damping mechanism is associated in this case with the so-called inverse Kirkendall effect [12].

In this work, we confine our consideration to a simplified account of vacancy sinks/sources, by assuming them "smeared" over the lattice, and their finite capacity is taken into account by introducing the average relaxation time of vacancies, τ, or the mean free path, L_V. In Section 2, we follow the basic ideas of the classical derivation by CH, but supplement the formulation by taking nonequilibrium vacancies into consideration. In so doing, we determine how the optimum period of a lamellar structure depends on L_V. In Section 3, we go beyond the scope of the linearity and one-dimensionality approximations and study the spinodal decomposition in a two-dimensional model for an arbitrary amplitude of concentration waves. We determine the time dependences for the characteristic heterogeneity length and a deviation of the concentration from its average value at various mean free paths of vacancies. We get convinced that the kinetics of spinodal decomposition is governed by two different, although interdependent, processes; namely, a change of the morphology (the topology of isoconcentration lines) and the very stratification of components at the given morphology. In this case, the finite capacity of vacancy sources and sinks really turns out to be an important factor for both processes (the topological and concentration ones).

2. Linear Approximation. One-dimensional Case

In this section, we confine the consideration to the initial stage of spinodal decomposition, when the amplitudes of the concentration stratification are much less than 1, so that the concentration waves can be regarded independent and all kinetic coefficients constant. By generalizing the known CH equations and taking the local gradients of vacancy concentrations into account, the component fluxes in the laboratory coordinate system can be written down in the form [6]

$$\Omega I_B = -(c_A D_B^* + c_B D_A^*)\frac{c_A c_B}{kT}\nabla\mu_{\text{ef}} + \\ + \frac{c_A c_B\,(D_B^* - D_A^*)}{c_V}\nabla c_V, \tag{1}$$

$$\Omega I_V = (D_B^* - D_A^*)\frac{c_A c_B}{kT}\nabla\mu_{\text{ef}} - \frac{(c_B D_B^* + c_A D_A^*)}{c_V}\nabla c_V, \tag{2}$$

where I_B and I_V are the flux densities of atoms B and vacancies, respectively, times the atomic volume (the dimensionality of those products is that of speed); c_B, c_A, and c_V are the atomic fractions of atoms B, A, and vacancies, respectively, with $c_B + c_A + c_V = 1$; k is the Boltzmann constant; T is the temperature; $\mu_{\text{ef}} = \frac{\partial g}{\partial c} - 2K\nabla^2 c_B$ is the chemical potential, which takes the nonlocal interactions in inhomogeneous alloys into account; K is the coefficient of the squared concentration gradient in the expression for the Gibbs potential density of an inhomogeneous alloy; and D_B^* and D_A^* are the intrinsic diffusion coefficients of atoms B and A, respectively. Equations (1) and (2) contain the cross terms, which describe the mutual influence of component B and vacancy fluxes. In particular, the second term in Eq. (1) describes the influence of nonequilibrium vacancies on the flux of B-atoms. This influence is governed by the difference between the intrinsic diffusion coefficients of components. The first term in Eq. (2) describes, on the contrary, the influence of the component mobility difference on the vacancy flux. Accordingly, the variations of B-component and vacancy concentrations in time are described by a continuity equation, which takes into account that the number of main-component atoms remains constant, whereas vacancies can disappear and emerge,

$$\frac{\partial c_B}{\partial t} = -\text{div}\,(I_B)\,, \tag{3}$$

$$\frac{\partial c_V}{\partial t} = -\mathrm{div}\,(I_V) - \frac{c_V - c_V^{\mathrm{eq}}}{\tau_V}. \quad (4)$$

One should bear in mind that Eq. (4) is written down in the relaxation approximation, i.e. the vacancy sources and sinks are considered to be "smeared" over the lattice.

At the initial stage of spinodal decomposition, the amplitude of a concentration wave can be adopted small. Consequently, Eqs. (3) and (4) can be linearized with regard for a spatial heterogeneity of only those quantities, which stand under gradients in Eqs. (1) and (2). Since the variations in the B-component and vacancy concentrations are interdependent now, it is natural, unlike the standard CH approach, to seek the solution of linearized Eqs. (3) and (4) in the form of **two** interdependent concentration waves,

$$c_B = A_B(t)\sin(kx), \quad c_V - c_V^{\mathrm{eq}} = A_V(t)\sin(kx). \quad (5)$$

Since the mobility of vacancies is much higher than that of atoms, it is reasonable to assume that the vacancy subsystem has enough time to follow slow variations of the main-component concentration. As a result, we can use a reduced description by imposing the quasistationarity condition on the vacancy concentration, $\frac{\partial c_V}{\partial t} \approx 0$. The substitution of this condition into Eq. (4) with regard for Eqs. (5) gives the following relation between the amplitudes of the vacancy and B-component concentrations:

$$A_V \cong A_B k^2 \frac{(D_B^* - D_A^*)\,\frac{c_A c_B}{k_B T}\left(g'' + \frac{2K}{L_V^2}(kL_V)^2\right)}{(kL_V)^2 + 1}. \quad (6)$$

The substitution of Eq. (6) into Eq. (3) in view of Eqs. (1) and (5) results in a simple differential equation for the amplitude of a concentration wave of component B,

$$\frac{dA_B}{dt} = R(k)A_B, \quad (7)$$

where

$$R(k) = -k^2(g'' + 2Kk^2)\frac{c_A c_B}{k_B T}\times$$

$$\times\left\{c_A D_B^* + c_B D_A^* - \frac{(D_B^* - D_A^*)^2}{c_V D_V} c_A c_B \frac{(kL_V)^2}{(kL_V)^2 + 1}\right\}. \quad (8)$$

Analogously to the standard CH theory, the solution of Eq. (7) has an exponential form,

$$A_B = \exp(R(k)t). \quad (9)$$

The concentration wave amplitude decreases if $R(k) < 0$ or grows if $R(k) > 0$.

However, besides the terms that are standard for the CH theory and include the second and fourth degrees of the wave number, the expression for $R(k)$ also contains a multiplier in the braces (see Eq. (8)). Its presence changes the position of the $R(k)$-curve maximum, which is the most pronounced at very small ratios between the partial diffusion coefficients. The most amazing difference of our results from the CH theory is obtained, if $r = D_A^*/D_B^* = 0$. In this case, the maximum of expression (8) can be found analytically, namely, the wave number k^*, at which the dependence $R(k)$ attains its maximum, equals

$$k^* = \frac{1}{L_V}\sqrt{\sqrt{\frac{L_V^2|g''|}{2K} + 1} - 1}. \quad (10)$$

In particular, if $\frac{L_V^2|g''|}{2K} \gg 1$ (i.e. the free path length of vacancies is large, and, respectively, their relaxation is slow), then $k^* \approx (1/L_V)\left(\frac{L_V^2|g''|}{2K}\right)^{1/4} = \left(\frac{|g''|}{2KL_V^2}\right)^{1/4}$. Recall that, according to the CH theory (in which the vacancy free path length tends to zero, being practically shorter than the period of a lamellar structure), the concentration wave with a different characteristic wave number, $k_{\mathrm{CH}}^* = \left(\frac{|g''|}{4K}\right)^{1/2}$, grows maximally rapidly. Hence, the ratio between the wave numbers of the concentration waves that grow most rapidly in those two limiting cases – absolutely inefficient sinks/sources and, on the contrary, perfectly efficient sinks/sources of vacancies – equals

$$\frac{k^*}{k_{\mathrm{CH}}^*} = \left(\frac{8K}{L_V^2|g''|}\right)^{1/4}. \quad (11)$$

By introducing the optimum length of a concentration wave from the CH theory, ratio (11) can be expressed in the form

$$\frac{\lambda_{\mathrm{CH}}^*}{\lambda^*} = \frac{1}{2^{1/4}\sqrt{\pi}}\sqrt{\frac{\lambda_{\mathrm{CH}}^*}{L_V}}. \quad (12)$$

Taking into account that the order of magnitude of the typical theoretical values for λ_{CH}^* is no more than tens of nanometers, and the mean free paths for vacancies amount to hundreds and thousands of nanometers, Eq. (12) testifies that, if either of the components is totally inertial at the vacancy diffusion, the periods of a lamellar structure have to be much longer than those predicted by the CH theory. In fact, the difference is

not so large. It diminishes very quickly, when the parameter $r = D_A^*/D_B^*$ deviates from zero. This can be seen from the plots of the dependence $\lambda^*(r)$ depicted in Fig. l, which were obtained by optimizing expression (8) at various mean free paths L_V. We see that the transition to the classical CH mode occurs at very small r-values and does not change any more after that.

3. Kinetics of Spinodal Decomposition in a Two-Dimensional Alloy. Nonlinearity Effects

Let us consider the kinetics of spinodal decomposition in a two-dimensional alloy at every stage of the process, by putting no restrictions concerning the linearity. Equations (1) and (2) for the fluxes remain invariable. The redistributions of atoms and vacancies are determined by the continuity equations

$$\frac{\partial c_B}{\partial t} = -\frac{\partial}{\partial x}(I_B) - \frac{\partial}{\partial y}(I_B), \tag{13}$$

$$\frac{\partial c_V}{\partial t} = -\mathrm{div}(I_V) - \frac{c_V - c_V^{\mathrm{eq}}}{\tau}. \tag{14}$$

The account of a finite capacity of sources and sinks of vacancies is carried out on a coarsened spatial scale (in the relaxation approximation). Remaining in the framework of the assumption concerning the quasistationarity of vacancies, but going beyond the linearity approximation, and taking the two-dimensional geometry of the problem into account, we obtain the following differential equation for the vacancy distribution at any fixed distribution of the basic component:

$$\nabla^2(c_V - c_V^{\mathrm{eq}}) - \frac{1}{L_V^2}(c_V - c_V^{\mathrm{eq}}) = \frac{1}{D_V}\mathrm{div}(\boldsymbol{\psi}), \tag{15}$$

where

$$\mathrm{div}(\boldsymbol{\psi}) = \frac{\partial}{\partial x}\left\{(D_B^* - D_A^*)\frac{c_A c_B}{k_B T}\frac{\partial}{\partial x}\times\right.$$

$$\left.\times\left(\frac{\partial g}{\partial c_B} - 2K\left[\frac{\partial^2 c_B}{\partial x^2} + \frac{\partial^2 c_B}{\partial y^2}\right]\right)\right\}+$$

$$+\frac{\partial}{\partial y}\left\{(D_B^* - D_A^*)\frac{c_A c_B}{k_B T}\frac{\partial}{\partial y}\times\right.$$

$$\left.\times\left(\frac{\partial g}{\partial c_B} - 2K\left[\frac{\partial^2 c_B}{\partial x^2} + \frac{\partial^2 c_B}{\partial y^2}+\right]\right)\right\}. \tag{16}$$

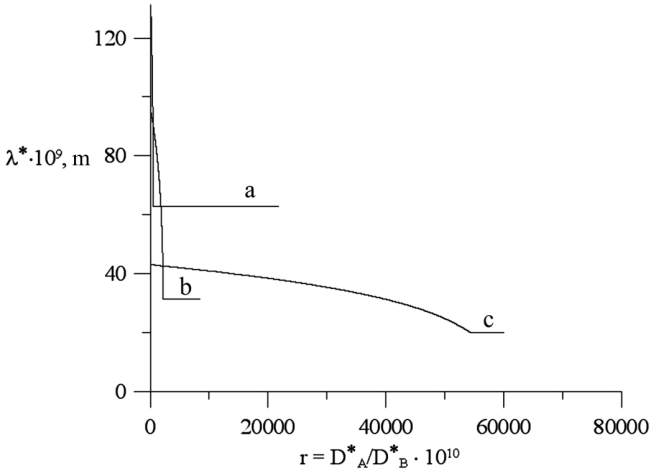

Fig. 1. Dependences of the optimum period in a lamellar structure on the ratio between the diffusion coefficients of labeled component atoms at $K = 10^{-37}$ J · m^2 and various mean free paths of vacancies: $L_V = 10^{-6}$ (*1*), 5×10^{-6} (*2*), and 10^{-7} m (*3*)

Certainly, the system of nonlinear equations (13) and (15) cannot be solved analytically. We obtained a solution numerically, using the explicit scheme for a finite-difference analog of Eq. (13) with the same space increment h along both axes and an iteration procedure for the determination of a vacancy field from Eq. (15). Specifically, Eq. (15) was written down in the finite-difference form including the new and previous iterations,

$$(c_V^n[i+1,j] + c_V^n[i-1,j] + c_V^n[i,j+1] + c_V^n[i,j-1]-$$

$$-4c_V^{n+1}[i,j])/(h^2) - \frac{c_V^{n+1}[i,j] - c_V^{\mathrm{eq}}}{L_V^2} = \frac{1}{D_V}(\mathrm{div}(\psi))_{i,j}^n,$$

whence

$$c^{n+1} = \left(c_V^n[i+1,j] + c_V^n[i-1,j] + c_V^n[i,j+1]+\right.$$

$$\left.+c_V^n[i,j-1] - \frac{h^2}{D_V}(\mathrm{div}(\psi))_{i,j}^n + \frac{h^2}{L_V^2}c_V^{\mathrm{eq}}\right) \Big/ \left(4 + \frac{h^2}{L_V^2}\right). \tag{17}$$

The iteration procedure is usually terminated, when a preset accuracy is achieved. This algorithm was applied to calculate the time evolution of the concentration fields for both B-component and vacancies.

To characterize a spatial heterogeneity of the system, we used the characteristic heterogeneity length, which

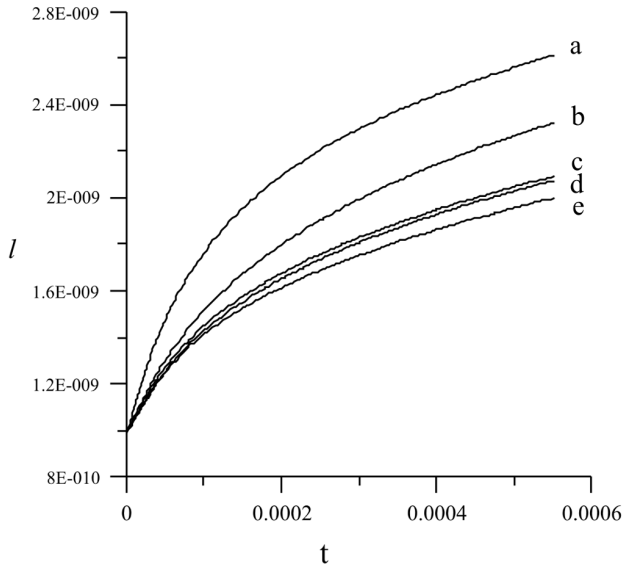

Fig. 2. Time dependence of the heterogeneity length at various relaxation times of vacancies $\tau = 10^{-8}$ (*1*), 10^{-7} (*2*), 5×10^{-7} (*3*), 10^{-6} (*4*), and 5×10^{-6} s (*5*). The values of other parameters are quoted in the text

was determined as follows:

$$\lambda = \sqrt{\frac{\sum\sum (c_B[i,j] - \bar{c}_B)^2}{\sum\sum \left[\frac{(c_B[i+1,j]-c_B[i-1,j])^2}{4h^2} + \frac{(c_B[i,j+1]-c_B[i,j-1])^2}{4h^2}\right]}}. \tag{18}$$

To characterize the decomposition degree (the degree of component separation), we used the deviation parameter dev, i.e. the root-mean-square deviation from the average value,

$$\text{dev} = \sqrt{\frac{\sum\sum (c_B[i,j] - \bar{c}_B)^2}{\sum\sum 1}}. \tag{19}$$

Evidently, the spinodal decomposition can be talked about only if the deviation is smaller than the half-width of the spinodal region.

One of our purposes was to compare the evolution kinetics of those two, just introduced parameters – "morphologic" and concentration ones. The calculations were carried out for the model of regular solid solution complemented with the nonlocal Cahn interaction,

$$g = \frac{z}{2}\left(c_A^2 \Phi_{AA} + c_B^2 \Phi_{BB} + 2c_B c_A \Phi_{AB}\right) +$$

$$+k_B T\left(c_A \ln c_A + c_B \ln c_B\right) + p(c_A \Omega_A + c_B \Omega_B) + 3k_B T,$$

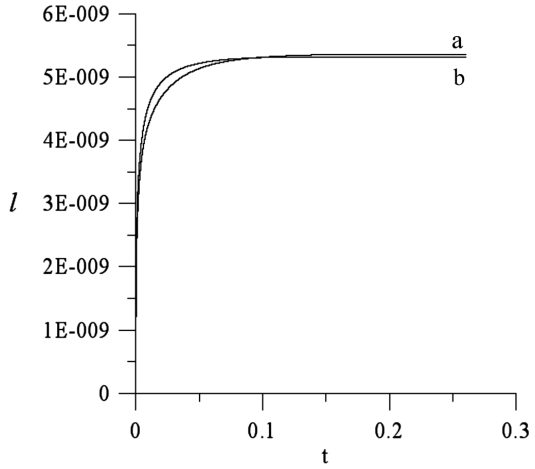

Fig. 3. Time dependence of the heterogeneity length at various times of vacancy relaxation $\tau = 10^{-7}$ (*1*) and 10^{-8} s (*2*)

where $\Phi_{AA} = \Phi_{BB} = -3\times10^{-20}$ J, $\Phi_{AB} = -1\times10^{-20}$ J, $T = 800$ K, $z = 12$, $\Omega_A = \Omega_B = \Omega = 2 \times 10^{-29}$ m^3, and $K = 6.26\times10^{-36}$ J $\cdot$ m^2. The selected value for the coefficient K in the gradient term is considerably larger than the values determined experimentally by G. Schmitz's group [13] for CuPy and AgCu systems. However, it enabled us to work with a coarser spatial mesh. The initial concentration was $c_{B0} = 0.5$ in this case. The diffusion coefficients of labeled atoms, provided the vacancy diffusion mechanism, are proportional to the vacancy concentration; therefore, they were introduced as the products $D^*_{A,B} = c_V K^*_{A,B}$. In this case, the kinetic coefficients K^*_A and K^*_B were determined by the formulas $K^*_A = K^*_{A0}\exp(\alpha_A c_B)$ and $K^*_B = K^*_{B0}\exp(\alpha_B c_B)$, where $K^*_{A0} = 10^{-11}$ m^2/s and $K^*_{B0} = 10^{-10}$ m^2/s were taken as constants, and $\alpha_A = \alpha_B = 0$.

The typical results of calculations are depicted in Fig. 2. As is seen, the alloy heterogeneity length grows at the initial stage more slowly for longer times of vacancy relaxation, i.e. for longer mean free paths of vacancies, i.e. for less efficient vacancy sinks/sources. It should be noted that the whole picture is typical of only early stages of the process. After long enough annealing times, every curve approaches an asymptote l_{as}, the magnitude of which depends on the Cahn parameter K, on the ratio between the diffusion coefficients, and, if this ratio is very small, on the mean free path of vacancies as well. It turned out that, to a good accuracy, $l_{\text{as}} = 1/k^*$, where k^* corresponds to the maximum point of $R(k)$ in formula (8) for the one-dimensional geometry. When this asymptotic length is achieved (see Fig. 3), the deviation still remains very small (of the order of 10^{-4}), i.e. the system is very far from the total decomposition.

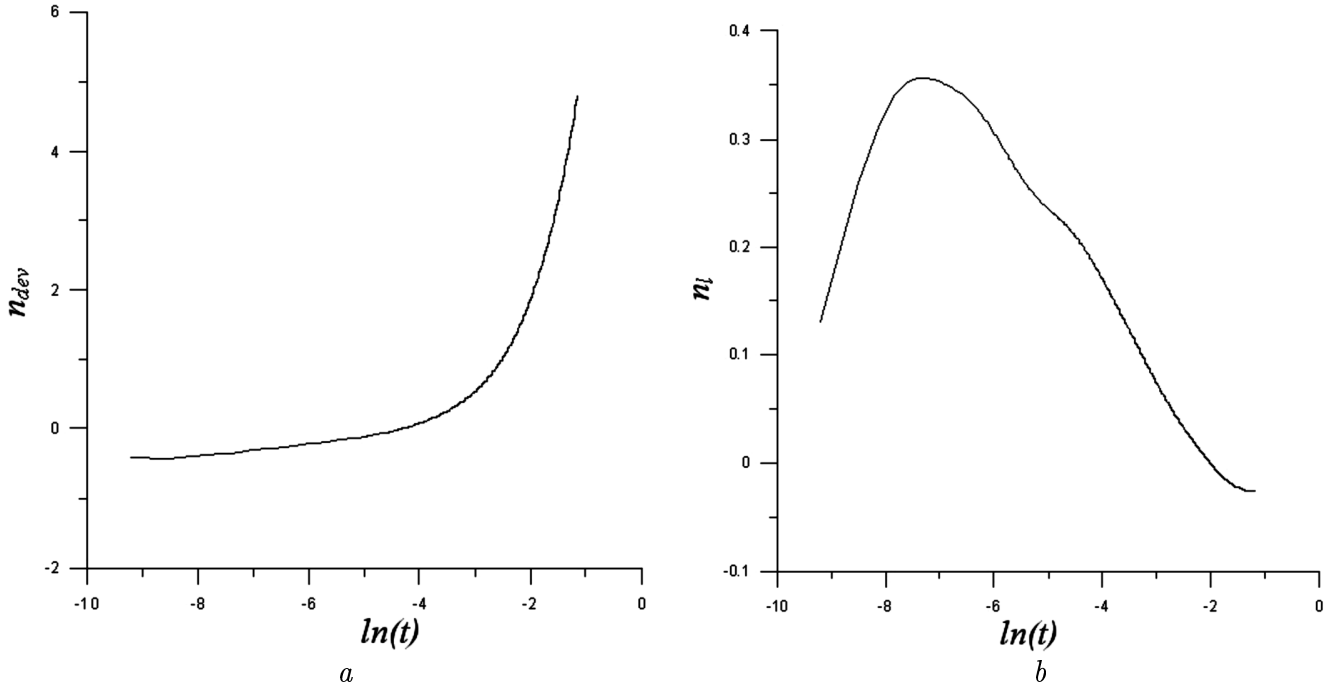

Fig. 4. Dependences of (*a*) separation degree growth indicator and (*b*) heterogeneity length growth indicator on the time on the logarithmic scale

Since the researches of the decomposition are always associated with a search for self-similar solutions at various stages, it is necessary that the dependences $\ln(l)$ versus $\ln(t)$ and $\ln(\mathrm{dev})$ versus $\ln(t)$ should be examined. The local tangents of the slope angles for corresponding plots determine the effective indicators of the growth rate for the heterogeneity length, $n_l = d\ln l/d\ln t$, and the component separation degree, $n_{\mathrm{dev}} = d\ln(\mathrm{dev})/d\ln t$, at various process stages. As Fig. 4 demonstrates, the indicator n_l increases at first and reaches a maximum at the intermediate stage of the process, whereas the indicator n_{dev} grows almost monotonously (to say nothing of a short process of regime establishment, when this indicator can turn out even negative). The maximum of the growth indicator depends, in particular, on K.

The decomposition kinetics depends also on the intensity of nonlocal interactions. As is seen from Fig. 5, a reduction of this parameter expectedly gives rise to the smaller values of heterogeneity length.

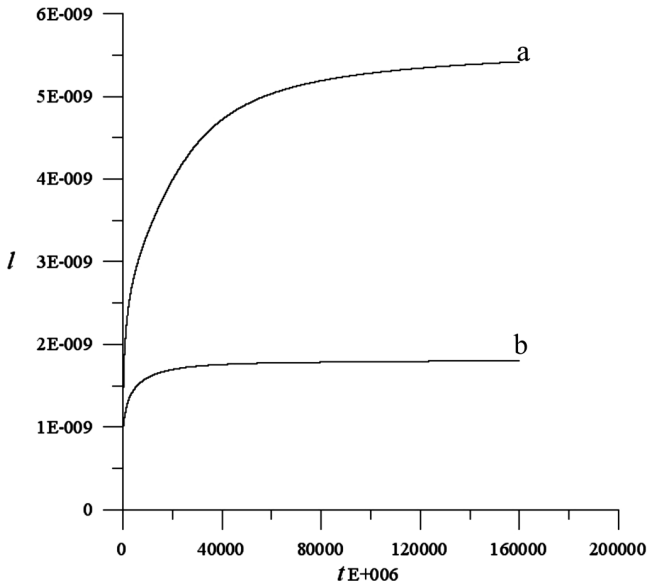

Fig. 5. Time dependences of the heterogeneity length at two various values of nonlocal interaction parameter $K = 10^{-36}$ (*1*) and 10^{-37} J $\times$ m^2 (*2*)

The increase of the deviation growth indicator in time means that the time dependence of a deviation is far from the power law. Instead, the logarithm of the deviation depends on the time almost linearly (Fig. 6), i.e. the deviation grows exponentially in our two-dimensional nonlinear model, just the same as it was in the linear one-dimensional model in Section 2. In other words, the establishment of a relatively stable topological pattern of isoconcentration lines does not at all mean the end of the spinodal decomposition: the decomposition con-

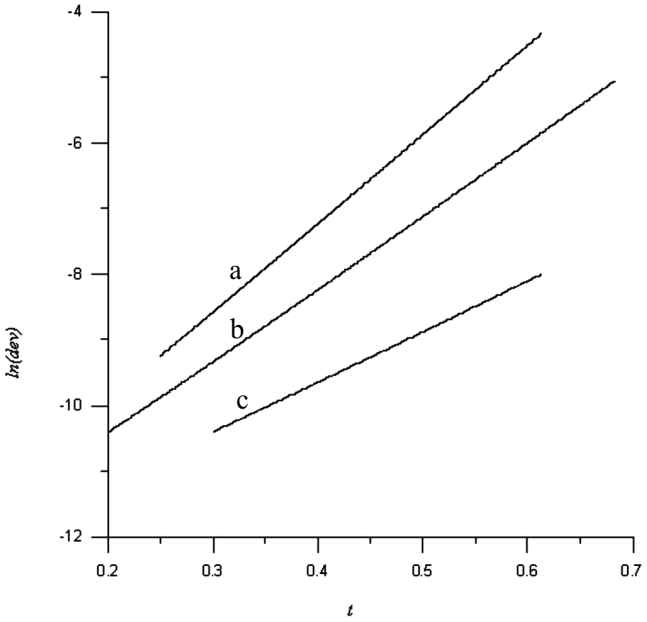

Fig. 6. Time dependences of the logarithm of the concentration deviation at various vacancy relaxation times $\tau = 5 \times 10^{-7}$ (*1*), 10^{-6} (*2*), and 5×10^{-6} s (*3*). All dependences are well approximated by straight lines $\ln(\mathrm{dev}) = R(k^*(L_V))t + \mathrm{const}$, where the $R(k^*(L_V))$-values coincide with those calculated by formula (8), provided that $k^* = 1/l_{\max}(L_V)$

tinues against the background of the topological "frame" that arises during the initial period of the process. This scenario is verified by the fact that the slopes of all three curves in Fig. 6 correspond to the values of quantity $R(k^*(L_V))$ obtained analytically from formula (8) for all three values of vacancy relaxation time. As was already said above, to a good accuracy, $k^* = 1/l_{\mathrm{as}}$ in this case.

4. Discussion of Results

The results presented above testify in favor of the following scenario for the spinodal decomposition kinetics in an alloy with a limited efficiency of vacancy sources and sinks. The initial fluctuation noise of the concentrations and the corresponding initial length of heterogeneity change rather slowly at the initial stage, with a value of growth indicator not exceeding a few hundredths. Then, the indicator of the heterogeneity length growth rate increases and reaches a maximum, the magnitude of which is of the order of $n_l \leq 0.25$ and weakly depends on the diffusion coefficient ratio and the mean free path of vacancies. After that, the growth of l is slowed down again, the indicator n_l approaches zero, and the heterogeneity length reaches a quasiasymptotic value, which remains almost constant for a long time, although the standard deviation of the components continues growing according to the exponential law e^{Rt}, where the parameter R practically coincides with the theoretical prediction (8) obtained in the framework of our linear one-dimensional model.

The magnitude of vacancy mean free path substantially affects the component separation kinetics: the larger the parameter L_V is, the more slowly the components are separated. However, the morphology of the system depends very weakly on the sink efficiency at real ratios between component mobilities. A sharp dependence appears only if either of the components is by several orders of magnitude more mobile than another one. In this case, the characteristic period of a lamellar structure is proportional to the square root of the vacancy mean free path. The topology of the system changes weakly at this stage, and the amplitude of the component separation grows.

We did not succeed in tracing the subsequent evolution of the system in the framework of the presented model, because a model with a nanometer spatial scale requires a lot of time for calculations. We may suppose that, at far stages, the system will develop by following ordinary coalescence laws, with a large volume fraction of both phases. The role of vacancy sinks/sources with a finite capacity in the course of coalescence has been analyzed rather recently [14].

The work was partially supported by the State Fund for Fundamental Researches of Ukraine in the framework of the joint Ukrainian–Russian project (grant F40.7/040).

1. M. Hillert, *Dr. Sci. thesis* (M.I.T., Cambridge, 1956).
2. J.W. Cahn and J.E. Hilliard, J. Chem. Phys. **28**, 258 (1958).
3. M.K. Miller, J.M. Hyde, M.G. Hetherington, A. Cerezo, G.D.W. Smith, and C. M. Elliott, Acta Materialia **43**, 3385 (1995); **43**, 3403 (1995); **43**, 3415 (1995).
4. L.S. Darken, Trans. AIME. **175**, 184 (1948).
5. S.Y. Hu and L.Q. Chen, Acta Materialia **52**, 3069 (2004).
6. A.M. Gusak, S.V. Kornienko, and G.V. Lutsenko, Defects Diffus. Forum **264**, 109 (2007).
7. A.V. Nazarov and K.P. Gurov, Fiz. Met. Metalloved. **37**, 496 (1974).
8. K.P. Gurov and A.M. Gusak, Fiz. Met. Metalloved. **59**, 1062 (1985).
9. A.M. Gusak, T.V. Zaporozhets, Yu.O. Lyashenko, S.V. Kornienko, M.O. Pasichnyy, and A.S. Shirinyan, *Diffusion-Controlled Solid State Reactions in Alloys,*

Thin Films and Nanosystems (Wiley-VCH, Berlin, 2010).

10. F.D. Fischer and J. Svoboda, Acta Mater. **58**, 2698 (2010).
11. M. Nastar, in *Abstracts of the 8-th International Conference on Diffusion in Materials DIMAT-2011* (Dijon, 2011), p. 25 [http://www.dimat2011.com/pdf/Book_IMAT.pdf].
12. A.D. Marwick, J. Phys. F **8**, 1849 (1978).
13. P. Stender, C.B. Ene, H. Galinski, and G. Schmitz, Int. J. Mater. Res. **99**, 480 (2008).
14. A.M. Gusak, G.V. Lutsenko, and K.N. Tu, Acta Mater. **54**, 785 (2006).

Received 19.05.11.
Translated from Ukrainian by O.I. Voitenko

РОЛЬ НЕРІВНОВАЖНИХ ВАКАНСІЙ У ПРОЦЕСІ СПІНОДАЛЬНОГО РОЗПАДУ

Н.В. Тютюнник, А.М. Гусак

Р е з ю м е

Загальноприйнята модель Кана–Хільярда для спінодального розпаду має принципову ваду, оскільки використовує наближення рівноважних вакансій, яке справедливе лише для процесів, характерна довжина яких суттєво більша за довжину вільного пробігу вакансій. Запропоновано схему врахування нерівноважного перерозподілу вакансій під час спінодального розпаду і його впливу на кінетику розпаду. На прикладі двовимірної системи проаналізовано ієрархію характерних часів еволюції морфології та концентрації у процесі спінодального розпаду.